European Journal of Medicinal Chemistry 285 (2025) 117244

Contents lists available at ScienceDirect

European Journal of Medicinal Chemistry

journal homepage: www.elsevier.com/locate/ejmech

Research paper

Functionalized regioisomers of the natural product phenazines myxin and iodinin as potent inhibitors of *Mycobacterium tuberculosis* and human acute myeloid leukemia cells

Goraksha Machhindra Khose [a], Siva Krishna Vagolu [b], Reidun Aesoy [c], Ísak Máni Stefánsson [a], Snorri Geir Ríkharðsson [a], Dagmar Ísleifsdóttir [a], Maonian Xu [a], Håvard Homberset [b], Tone Tønjum [b,d], Pål Rongved [e], Lars Herfindal [c], Elvar Örn Viktorsson [a,*]

[a] School of Health Sciences, Faculty of Pharmaceutical Sciences, University of Iceland, Hofsvallagata 53, IS-107, Reykjavik, Iceland
[b] Unit for Genome Dynamics, Department of Microbiology, University of Oslo, N-0316, Oslo, Norway
[c] Centre for Pharmacy, Department of Clinical Science, University of Bergen, Jonas Lies vei 87, N-5021, Bergen, Norway
[d] Unit for Genome Dynamics, Department of Microbiology, Oslo University Hospital, N-0424, Oslo, Norway
[e] School of Pharmacy, Department of Pharmaceutical Chemistry, University of Oslo, PO Box 1068 Blindern, N-0316, Oslo, Norway

ARTICLE INFO

Keywords:
Phenazine 5,10-dioxides
Mycobacterium tuberculosis
Acute myeloid leukemia
Structure-activity relationships (SAR)
Cellular toxicity studies

ABSTRACT

The natural bioactive products myxin and iodinin are phenazine 5,10-dioxides possessing potent anti-bacterial and anti-cancer activity in vitro. This work describes the synthesis and derivatization of new myxin and iodinin regioisomers, developed from 1,3-dihydroxyphenazine 5,10-dioxide. Compounds were evaluated for activity towards *M. tuberculosis* (*Mtb*) strains, a human AML cell line (MOLM-13), and two non-cancerous mammalian cell lines (NRK and H9c2). Highly potent analogs were developed having IC_{50} values against MTB down to 20 nM and 1.4 μM for human AML cells. 1-OH-3-*O*-alkyl substituted derivatives demonstrated high efficacy against *Mtb* and low toxicity in normal cells. 2,3-substituted regioisomers of myxin and iodinin were shown to be inactive, highlighting the importance of oxygen substituent in position 1 of the scaffold. A strong positive correlation between anti-MTB and anti-AML activity was revealed, suggesting a common mechanism of action in bacteria and cancer cells. These findings demonstrate the therapeutic potential of 1,3-*O*-functionalized phenazine 5,10-dioxides in chemotherapy for *Mtb* and AML and contribute to the structure-activity understanding of phenazine 5,10-dioxides with respect to their biological activity.

1. Introduction

New antimicrobial agents are urgently called for to counteract the fast development of antimicrobial resistance (AMR). One form of response involves the development of natural products that offer antimicrobial modes of action priorly untouched in terms of clinical use.

A significant part of the global AMR problem can be attributed to tuberculosis (TB) caused by *Mycobacterium tuberculosis* (*Mtb*). The rise of both multidrug resistant (MDR) and extensively drug resistant (XDR) strains of *Mtb* are also of special concern. In 2023, WHO as part of the *Global research agenda for AMR in human health,* outlined 40 research priorities on AMR out of which 7 directly addressed drug-resistant *Mtb*. [1] The 2024 WHO Global tuberculosis report gave estimates of 10.8 million new cases and 1.25 million deaths in 2023 (161 thousand of which were HIV positives) [2]. To highlight the situation's severity even further, more than 480 thousand new cases of rifampicin-resistant TB were reported in 2022 [1]. Antitubercular chemotherapies are particularly challenging since the standard therapeutic protocols against sensitive *Mtb* strains involve combinations of several antibiotic drugs [3]. For instance, the standard rifampicin (RIF), isoniazid (INH), pyrazinamide and ethambutol (RIPE) treatment last for 6–9 months. A newer and shorter alternative lasts for four months with combined intake of rifapentine, moxifloxacin, INH and pyrazinamide [3]. In cases where the pathogen is resistant to any of these drugs, the therapies are more complex, prolonged, and expensive – involving the use of less attractive drugs in terms of toxic side effects and drug administration. MDR-TB strains are defined as being resistant to the two cornerstones of anti-TB therapies through the past decades: INH or RIF. XDR strains are

* Corresponding author.
E-mail address: eov@hi.is (E.Ö. Viktorsson).

https://doi.org/10.1016/j.ejmech.2025.117244
Received 17 November 2024; Received in revised form 20 December 2024; Accepted 3 January 2025
Available online 4 January 2025

even more serious, defined as resistant to not only INH or RIF, but also to all fluoroquinolones and at least one 2nd line anti TB-drug. Examples of 2nd line drugs include levofloxacin, moxifloxacin, capreomycin, bedaquiline, telacebec (Q203), delamanid, linezolid and pretomanid [4].

Phenazines are aromatic natural products originating from the shikimic acid pathway in bacteria (see structure, Fig. 1). Several reviews have already highlighted their biological occurrence, function, biosynthesis and strategies for synthesis [5–7]. In 2017, the isolation and characterization of more than 180 different phenazine natural products was reported [5]. Fig. 1 shows the phenazine core (**1**) and selected examples of phenazine natural products.

Pyocyanin (**2,** Fig. 1) was isolated in 1859 and is generally referred to as the best-known and most extensively studied phenazine to date [7]. The role of pyocyanin as a virulence factor of *Pseudomonas aeruginosa* has been a topic of interest due to its abilities to cause cytotoxicity and immune suppression in host tissue cells, and also to promote enhanced virulence of the pathogen [8–10]. The deep purple pigment iodinin (**5,** Fig. 1) was harvested by Davies in 1939 from cultures of *Brevibacterium iodinum* [11]. It exhibits weak or moderate antimicrobial potency and very poor aqueous solubility, the latter as a result of two intramolecular ion-dipole bonds [12]. Isolation of myxin (**6**), a more potent and broad spectrum phenazine antimicrobial agent of cherry-red color was described in 1966 from *Lysobacter antibioticus* by Peterson et al. (first attributed to *Sorangium* spp.) [13,14]. Our group has previously shown that iodinin (**5**), myxin (**6**) and synthetic phenazine derivatives have the potential to become an alternative in chemotherapy for acute myeloid leukemia (AML) [15,16]. Among natural phenazines, the structures of iodinin (**5**) and myxin (**6**) are particularly noteworthy as they both contain a set of heterocyclic aromatic *N*-oxides in positions 5 and 10 (Fig. 1). These types of functional groups rarely occur in natural products [17] and add to the complexity concerning modes of action.

Several modes of action should be considered for every individual phenazine. *Firstly*, phenazines can undergo redox-cycling processes. Gates et al. demonstrated how 1-hydroxyphenazine (**3**, Fig. 1), a virulence factor of *P. aeruginosa* can catalyze the production of ROS upon bioreductive processes [18]. Consequently, these types of phenazines (1-OH substituted) are considered able to deplete intracellular storage of antioxidants through continuous production of superoxide ($O_2^{\bullet-}$) from molecular oxygen (O_2). *Secondly*, some phenazines including iodinin (**5**) and myxin (**6**) have been shown to intercalate between DNA-base pairs and interrupt normal DNA-metabolism [19–21]. The planar aromatic moiety of anthracycline anticancer agents like doxorubicin and daunorubicin have structural resemblance to that of iodinin (**5**) and myxin (**6**). *Thirdly,* phenazines have the possibility to chelate metals. For instance, 1-hydroxyphenazine (**3**) is a proven metal chelator and can starve cultures of *Aspergillus fumigatus* from iron [22]. The antibiotic Lomofungin (**4**, Fig. 1) has also been shown to chelate Zn^{2+} [23,24]. 8-Hydroxyquinoline (structure not shown) is a chelator of bivalent cations [25], a scaffold hardwired into many natural 1-OH functionalized phenazines. *Fourthly;* phenazine 5,10-dioxides like myxin are known to unleash the highly cytotoxic $^{\bullet}OH$ radical upon intracellular reduction, which can abstract protons from the deoxyribose backbone of DNA and cause DNA-strand breaks [26]. Several antineoplastic antibiotics used in the clinic, including the anthracyclines, mitomycin and bleomycin are known to act by related mechanisms. The anthracyclines are among the most extensively used chemotherapeutic agents used for cancer treatment and continue to play a crucial role in the treatments of various malignant disorders, including leukemia, lymphomas (Hodgkin's and non- Hodgkin's), ovarian-, thyroid-, and breast cancers. Although highly effective chemotherapeutic agents, the anthracyclines are also infamous for dose-dependent cardiotoxicity [27,28].

Phenazines are well-known to possess antimicrobial activities. Weigele et al. reported in 1970 a structure-activity relationship (SAR) study on myxin (**6**) and semisynthetic derivatives [29]. Patents on phenazine 5,10-dioxides were also acquired [30,31]. More recently, Huigens and colleagues provided excellent reports on the synthesis and SAR-studies on halogenated phenazines derived from 1-hydroxyphenazine (**3**) and its marine natural analog 2-bromo-1-hydroxyphenazine [32–35]. These studies included antimicrobial activities against *Mtb* and other pathogens. The same group has also demonstrated the potent biofilm-eradicating effects of multiple halogenated phenazines [32]. However, no phenazine 5,10-dioxides were included in these studies. Conda-Sheridan et al. also investigated analogs of 2-bromo-1-hydroxyphenazine as chemopreventive agents [36]. The team of Cerecetto and González has also investigated phenazine 5,10-dioxides as hypoxia-selective cytotoxins for antineoplastic activities [37–41]. Importantly, the same group also reported an in vivo study showing treatment with phenazine 5,10-dioxides to reduce tumor volumes [40].

The aims of this study were to synthesize a set of phenazine 5,10-dioxides, and to explore and demonstrate the potential of this compound class to inhibit virulent strains of *Mtb* and cancerous cells. The choice of pursuing 1,3-dihydroxyphenazine 5,10-dioxide as a lead scaffold was based on the following considerations: 1) This scaffold has shown antimicrobial potential [31]. 2) The 1,3-bis-*O*-substituted scaffold is easily accessed in one synthetic step in gram quantities from inexpensive starting materials, providing access to interesting regioisomers of the natural antibiotics iodinin (**5**) and myxin (**6**). Since we considered this class of compounds to act as antineoplastic antibiotics, we tested them against a human AML cell line. The compounds were also evaluated in terms of cellular toxicity in non-malignant mammalian host cell lines (NRK and H9c2). We have previously reported an efficient total synthesis method for both iodinin (**5**) and myxin (**6**), and the synthesis and biological evaluation of multiple derivatives [15,16].

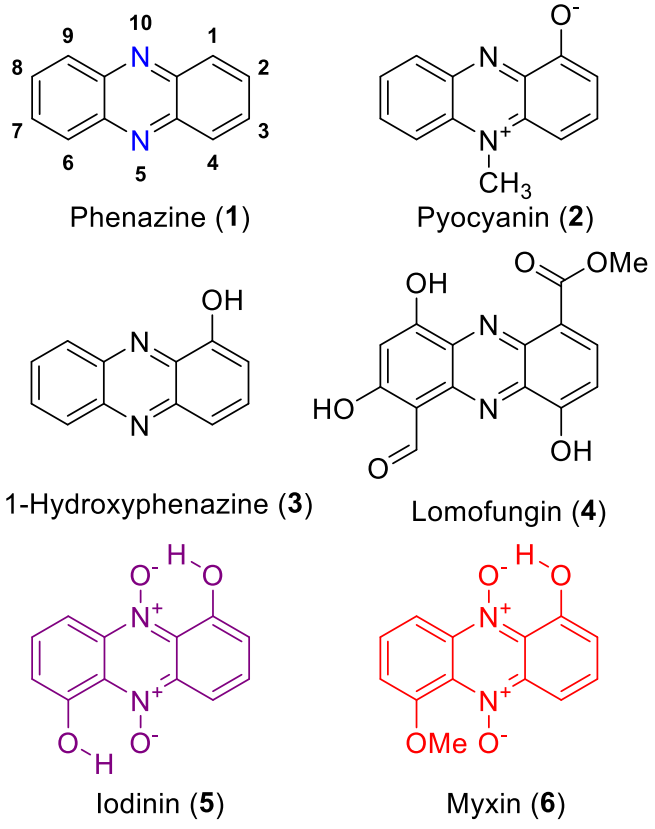

Fig. 1. Phenazine (**1**) and selected natural products including pyocyanin (**2**), 1-hydroxyphenazine (**3**), lomofungin (**4**), iodinin (**5**) and myxin (**6**).

2. Results and discussion

2.1. Synthesis of compounds

1,3-Dihydroxyphenazine 5,10-dioxide (**7**), a regioisomer of the antibiotic iodinin (1,6-dihydroxyphenazine 5,10-dioxide, **5**) was secured from a Beirut-type reaction where benzofuroxan and phloroglucinol were condensed in an aqueous NaOH dispersion at room temperature (Scheme 1) [31,42]. This method proved scalable to a multi-gram scale and involved no chromatographic purification steps. Excellent purity judged by ^{1}H NMR and HPLC could be achieved by simple washing with solvents after filtration (Scheme 1).

One of the primary aims was also to explore two possible 1,3-substituted regioisomers of the antibiotic myxin (**6**) derived from compound **7**. These were 1-hydroxy-3-methoxyphenazine 5,10-dioxide (**8**) and 3-hydroxy-1-methoxyphenazine 5,10-dioxide (**13**) (structures shown in Scheme 1). First, the synthesis of (**8**) was achieved by a single methylation step on **7** using MeI and K_2CO_3/18-Crown-6 in DMF in line with prior methods used to yield myxin (**6**) from iodinin (**5**) [15,16]. Also, the bis-*O*-methylated analog 1,3-dimethoxyphenazine 5,10-dioxide (**9**) could be isolated from an entry using higher molar equivalents of the methylating agent when KO*t*Bu was explored as a base. The corresponding ethyl derivative (**10**) was also prepared from **7** using EtI instead of MeI (Scheme 1). Thereafter, our focus was turned towards the other possible regioisomer of myxin, 3-hydroxy-1-methoxyphenazine 5,10-dioxide (**13**, Scheme 1). To selectively methylate 1-OH of the scaffold, installment of a protecting group onto 3-OH was first undertaken. This stems from higher nucleophilicity of the 3-OH position compared to 1-OH of **7**, at least partly because 1-OH is intramolecularly bound with ion-dipole forces between the phenol hydrogen in position 1 and the adjacent aromatic *N*-oxide placed in position 10 (structure **7**, Scheme 1). This intramolecular bond can clearly be observed in the ^{1}H NMR spectra for compound **7**, as chemical shift for the 1-OH arrives at 14.96 ppm, while the 3-OH chemical shift arrives at 11.20 ppm in DMSO-d_6 (See NMR, Fig. S-3, supplementary information). For the phenol protection of 3-OH, we chose to utilize EOM-Cl, a less toxic variant of the more commonly used MOM-Cl. This reaction gave 55 % yield of **11** after column purification (Scheme 1). Subsequently, the 1-OH phenol was methylated to give **12** (see Scheme 1). The EOM-protecting moiety was then conveniently cleaved by exposure of **12** to TFA in DCM (1:1). During this deprotection protocol, **13** precipitated and could be collected conveniently in high purity by a simple filtration of the reaction mixture. Although compounds **8** and **13** are regioisomers, their physicochemical properties differ since an intramolecular bond can only be formed within compound **8**. Therefore, the regioisomer **13** is more polar than **8** enhancing its aqueous solubility.

As our in vitro studies progressed further and potent biological activities of EOM-analog **11** were revealed, the corresponding 3-MOM derivative **14** was also synthesized and screened for activity. The literature known compound 1-methoxyphenazine 5,10-dioxide (**16**) was also included to our study since a report from 1970 by Leimgruber et al. demonstrated the antimicrobial potency and spectrum to be quite similar to the antibiotic myxin (**6**) [29]. This compound was prepared by methylation of 1-hydroxyphenazine 5,10-dioxide (**15,** Scheme 2), the synthesis of which has previously been reported by this group [16] and others [42].

Other derivatives were prepared from the lead scaffold. Exposure of **7** to ethyl bromoacetate and K_2CO_3/18-Crown-6 resulted in 3-positioned 2-ethoxy-2-oxoethoxy compound **17** after recrystallization (Scheme 3). Also, the corresponding 1,3-*O*-bis substituted analog **18** was isolated from another entry after column purification (Scheme 3). Moreover, two methoxy regioisomers were prepared with the above-mentioned side

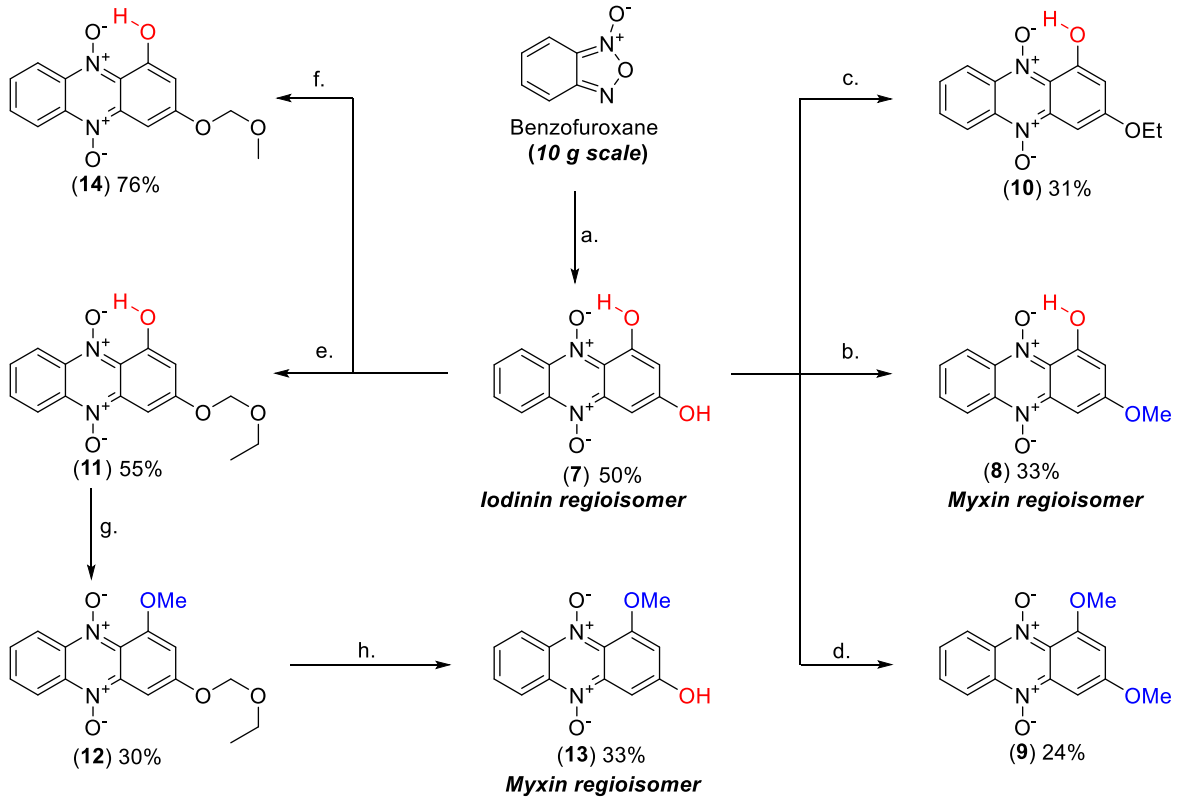

Scheme 1. Synthesis outline for the synthesis of 1,3-dihydroxyphenazine 5,10-dioxide (**7**) and derivatives, including the myxin regioisomers **8** and **13**. Reaction conditions: a) Phloroglucinol, NaOH (cat.), H_2O, rt, 16 h, 50 %. b) MeI, K_2CO_3, 18-Crown-6, DMF, rt, 16 h, 33 %. c) EtI, K_2CO_3, 18-Crown-6, DMF, rt, 16 h. d) MeI, KOtBu, 18-Crown-6, DMF, 0 °C to rt, 16 h. e) EOM-Cl, K_2CO_3, 18-Crown-6, DMF, rt, 16 h. f) MOM-Cl, K_2CO_3, 18-Crown-6, DMF, rt, 16 h. g) MeI, K_2CO_3, 18-Crown-6, DMF, rt, 16 h. h) TFA, DCM, 0 °C, 3 h.

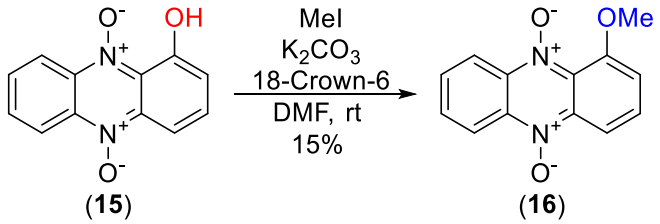

Scheme 2. The synthesis of 1-methoxyphenazine 5,10-dioxide (**16**).

chain (2-ethoxy-2-oxoethoxy), either with a methoxy group in position 1 or 3 on the scaffold. First, 3-(2-ethoxy-2-oxoethoxy)-1-methoxyphenazine 5,10-dioxide (**19**) was obtained after a one-pot procedure was undertaken on **7**, first exposing it to ethyl bromoacetate, then MeI. Column purification gave 30 % yield of **19** using this method. Next, the reversed analog of **19**, 1-(2-ethoxy-2-oxoethoxy)-3-methoxyphenazine 5,10-dioxide (**20**) was isolated with column purification and recrystallization after the exposure of **8** to ethyl bromoacetate (See Scheme 3). Thus, a total of 4 different 2-ethoxy-2-oxoethoxy analogs were successfully synthesized. The rational for selecting this functional group was that 2-ethoxy-2-oxoethoxy analogs of iodinin proved to possess highly potent antileukemic activities as reported previously by this group (compound 15 in ref. 15, compound 7 in ref. 16) [15,16].

Acetylation of the phenols were investigated (Scheme 3) to explore the biological activities of simple aromatic esters in vitro. Acetyl chloride with pyridine in DCM gave the 3-monosubstituted derivative **21** in 10 % yield. Similarly, the 1,3-*O*-bis acetylated compound **22** was also reached in 13 % yields. The 1-OH of the myxin regioisomer **8** (Scheme 3) was also exposed to acetyl chloride and pyridine, acquiring **23** in 11 % yield. Thus, all attempted acetylation reactions resulted in poor yields (11–13 %) due to formation of multiple byproducts as judged by TLC. Consequently, multiple chromatographic steps were required for each of these derivatives to obtain high purity. However, sufficient milligram quantities of **21**–**23** were secured for in vitro studies.

Lastly, two more compounds with a 2,3-substitution pattern were synthesized and included in our in vitro studies. 2,3-Dihydroxyphenazine 5,10-dioxide (**24**) was isolated after benzofuroxan was exposed to catechol in 15 % EtOH/KOH (Scheme 4). The reaction gave only 17 % yield. This compound is a regioisomer of both iodinin (**5**) and **7**, and as such of high interest in terms of SAR observations. Similarly, a Beirut reaction between benzofuroxan and 2-methoxyhydroquinone gave 2-hydroxy-3-methoxyphenazine 5,10-dioxide (**25**) in good yield of 75 %. Compound **25** is a regioisomer of myxin (**6**), **8** and **13**.

2.2. Antitubercular activity

Antimycobacterial activity for all compounds was assessed against the *Mtb* virulent reference strain H37Rv by applying the Microplate Alamar Blue Assay (MABA) protocol. Half maximal inhibitory concentration (IC_{50}) values against the H37Rv strain are presented in Table 1. For all compounds with IC_{50} of 1000 nM or less, studies were also performed on three different *Mtb* clinical isolates expressing resistance genes for INH or RIF (KatG+, InhA+, rpoB+).

The experiments revealed that myxin had potent antitubercular activity (IC_{50}: 14 nM). Also, compound **16**, which has been previously shown to exhibit potent activity against a variety of other pathogens (not *Mtb*) [29], showed a potent IC_{50} as well (40 nM). Myxin (**6**) outperformed compound **16** in terms of being less toxic towards the normal

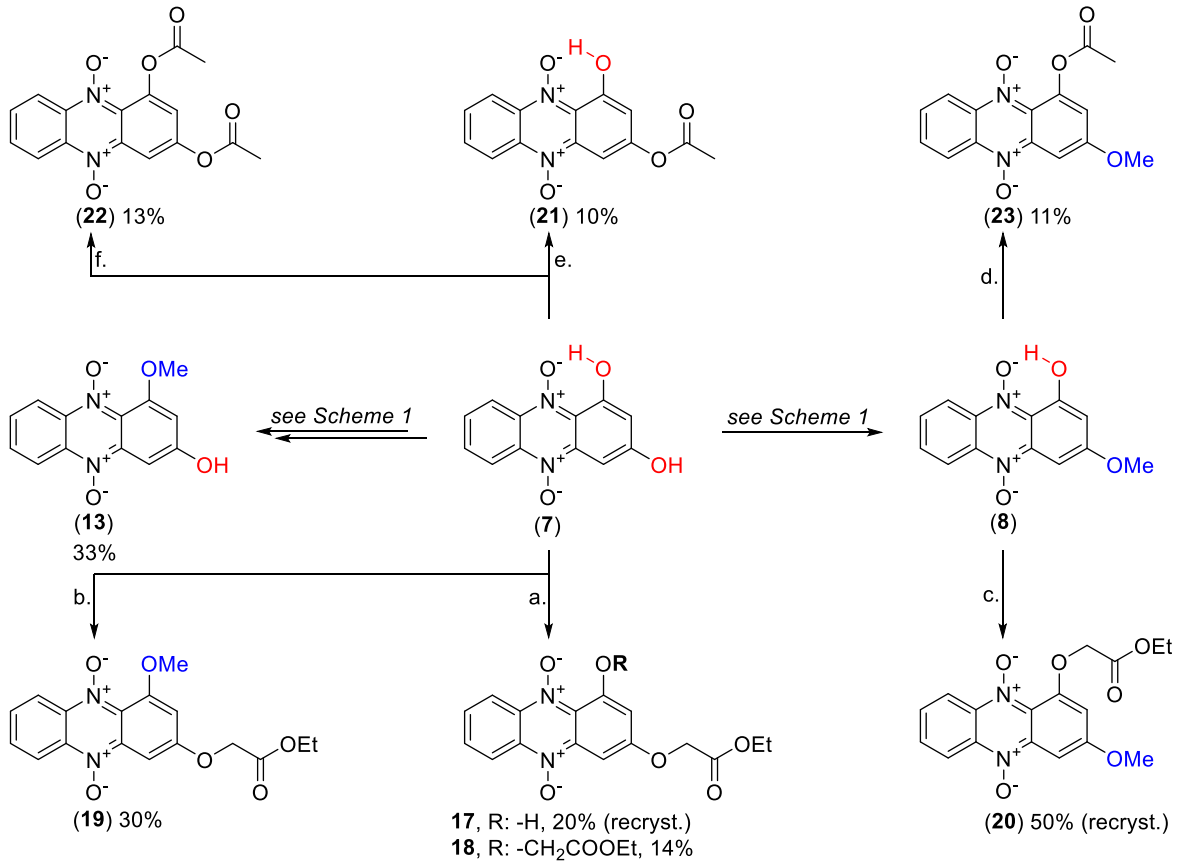

Scheme 3. Synthesis outline for analog series from **7** and **8** and reaction conditions: a) ethyl bromoacetate, K_2CO_3, 18-Crown-6, DMF, rt, 16 h. b) ethyl bromoacetate, K_2CO_3, 18-Crown-6, DMF, rt, 8 h, then MeI, rt, 8 h. c) ethyl bromoacetate, K_2CO_3, 18-Crown-6, DMF, rt, 16 h. d) acetyl chloride, pyridine, DMAP, DCM, 0 °C to rt, 16 h. e) acetyl chloride, pyridine, DCM, 0 °C to rt, 16 h. f) acetyl chloride, pyridine, DCM, 0 °C to rt, 16 h.

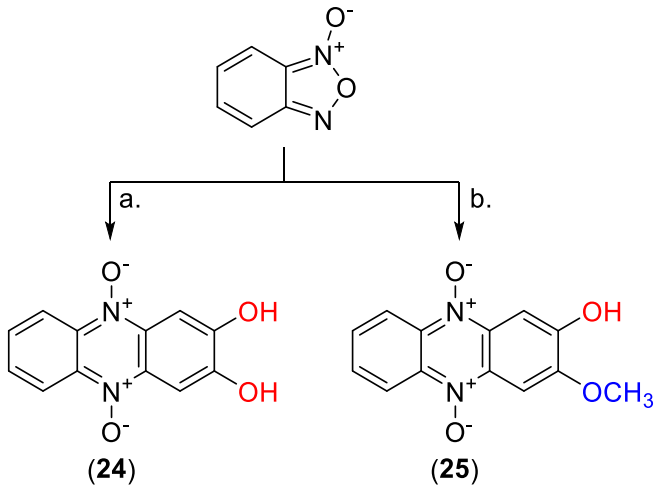

Scheme 4. Synthesis outline and reaction conditions for the compounds **24** and **25**. a) catechol, 15 % KOH/EtOH, rt, overnight (17 %). b) 2-methoxyhydroquinone, NaOH (cat.), H_2O, 1h, rt (75 %).

cell lines NRK and H9c2 (Table 1 and Fig. 2A and B).

Six new derivatives were also found to possess IC_{50} values in the range of 20–80 nM against H37Rv. These were **8**, **10**, **11**, **12** and **23**. Among the new derivatives, **11** was the most effective compound (IC_{50}: 20 nM), similar to myxin (14 nM). Among the most active compounds, **10** and **11** exhibited better anti-tubercular potency against the drug–resistant *Mtb* strain with *inhA* promoter mutation as compared to other compounds (Table 1). Importantly, these compounds were also generally well tolerated by the normal cell lines NRK and H9c2. As an example, compound **10** with an IC_{50} of 40 nM against H37Rv had IC_{50} values of 87- and 103 μM in NRK and H9c2, respectively. Thus, over 2000-fold difference in concentration between IC_{50} of the pathogen and IC_{50} for NRK, and even more difference for H9c2. Fig. 2A summarizes the structures of the six most active compounds tested against H37Rv.

2.3. Cytotoxicity towards mammalian cell lines

The cytotoxic activity of the myxin/iodinin regioisomers and derived compounds was tested on the acute myeloid leukemia cell line (MOLM-13) in order to examine their potential as chemotherapeutic agents. As a control of their possible cellular toxicity, the compounds were additionally tested on two cell lines derived from normal tissue: kidney epithelial cells (NRK) and cardiomyoblasts (H9c2). Table 1 shows the results from the tests on mammalian cells expressed as the concentration giving a 50 % reduction in metabolic activity (IC_{50}, sometimes referred to as EC_{50}). The compounds were first tested on MOLM-13 cells, and those exhibiting an IC_{50} value below 10 μM were further tested on NRK and H9c2 cells.

The most potent compounds, showing an IC_{50} of 2 μM or lower towards MOLM-13 were **10**, **16**, **18**, and **20**. In general, the AML cells were more sensitive to all the compounds compared to the two normal cell lines (paired samples *t*-test, significance: 0.008 MOLM-13 vs. NRK and 0.002 MOLM-13 vs. H9c2). The two normal cell lines did not differ in sensitivity to the compounds (paired samples *t*-test, no significance: $p = 0.94$, Supplementary Figs. S–1). Of the compounds with high activity towards MOLM-13, **10** and **18** showed particularly low activity towards normal cell lines (Table 1 and Fig. 2).

When comparing the response of the *Mtb* strain H37Rv with that of the MOLM-13 cells, it was shown that the H37Rv were more sensitive to these compounds than the MOLM-13 cells (paired samples *t*-test, significance: 0.035, Supplementary Figs. S–1). Still, there was a non-linear correlation between the efficacy towards H37Rv and MOLM-13 cells (Spearman's Rho: 0.63, 2-tailed significance: 0.002). However, compounds **18** and **20** deviated from this pattern (Supplementary Figs. S–2), in that these showed very high potency towards MOLM-13 cells (2.0 and 1.4 μM, respectively), but had low efficiency towards H37Rv (2880 and 2410 nM). Structurally, both **18** and **20** share a 2-ethoxy-2-oxoethoxy functional group in position 1 of the phenazine scaffold. We have earlier demonstrated several highly potent antileukemic phenazine analogs possessing this side chain in position 1 [15,16]. Without these two compounds, the correlation between the response of the H37Rv strain

Table 1
IC_{50} values (±SEM) of phenazine 5,10-dioxide analogs on drug-sensitive (H37Rv) and clinical isolates of *Mycobacterium tuberculosis* and the cell lines MOLM-13, NRK and H9c2.

	M. tuberculosis				Mammalian cell lines		
	H37Rv *Drug-sensitive*	katG+ *INH-resistant*	inhA+ *INH-resistant*	rpoB+ *Rifampicin-resistant*	MOLM-13 Human leukemia	NRK Rat kidney epithelial	H9c2 Rat cardiomyoblast
Cpd#	IC_{50} (nM)	IC_{50} (nM)	IC_{50} (nM)	IC_{50} (nM)	(IC_{50} μM)	(IC_{50} μM)	(IC_{50} μM)
5 (iodinin)	170 ± 5	70 ± 20	n.d	n.d	2.0 ± 0.07[a]	>50[a]	>50[a]
6 (myxin)	14 ± 3.2	62.5	62.5	62.5	1.4 ± 0.30[a]	77 ± 11[a]	46 ± 4.1[a]
7	560 ± 150	500	125	1000	11 ± 1.9	n.d.	n.d.
8	50 ± 10	62.5	16	62.5	3.8 ± 0.72	38 ± 4.7	81 ± 11
9	120 ± 20	125	125	125	6.0 ± 0.76	46 ± 5.7	108 ± 22
10	40 ± 4.0	62.5	4	62.5	2.0 ± 0.21	87 ± 9.4	103 ± 22
11	20 ± 2.4	62.5	4	31.2	3.8 ± 0.37	>25	>25
12	60 ± 10	62.5	31.2	31.2	5.1 ± 0.45	>25	>25
13	1910 ± 200	n.d.	n.d.	n.d.	>100	>100	>200
14	110 ± 10	125	125	125	5.2 ± 0.54	>100	>50
15	260 ± 40	50 ± 10	n.d	n.d	11 ± 1.8[a]	79 ± 4.2[a]	>100[a]
16	40 ± 4.0	125	125	125	1.4 ± 0.07	32 ± 6.9	12 ± 3.0
17	170 ± 20	250	62,5	250	5.7 ± 1.13	194 ± 14	89 ± 8
18	2880 ± 270	n.d.	n.d.	n.d.	2.0 ± 0.31	>200	>200
19	250 ± 100	250	250	250	10 ± 1.150	n.d.	n.d.
20	2410 ± 100	n.d.	n.d.	n.d.	1.4 ± 0.15	14 ± 1.4	19 ± 1.5
21	850 ± 120	1000	500	1000	16 ± 1.3	n.d.	n.d.
22	5001 ± 149	n.d.	n.d.	n.d.	35 ± 2.6	n.d.	n.d.
23	80 ± 10	125	125	250	6.5 ± 0.29	36 ± 3.6	55 ± 6.7
24	>50,000	n.d.	n.d.	n.d.	>50	n.d	n.d
25	11,100 ± 420	n.d	n.d	n.d	>100[b]	n.d	n.d

The IC_{50} values were obtained after 1 week incubation (*M. tuberculosis*) or 24 h incubation (mammalian cell lines). Viability was assessed by measurement of metabolic activity using resazurin (*M. tuberculosis*) or the formazan-based WST-1 assay (mammalian cell lines). See Methods section for details on experimental conditions and calculations of IC_{50} values. The data are average of 2–5 experiments. ± Std error. [a]IC_{50} values according to Viktorsson et al., 2021.[14].

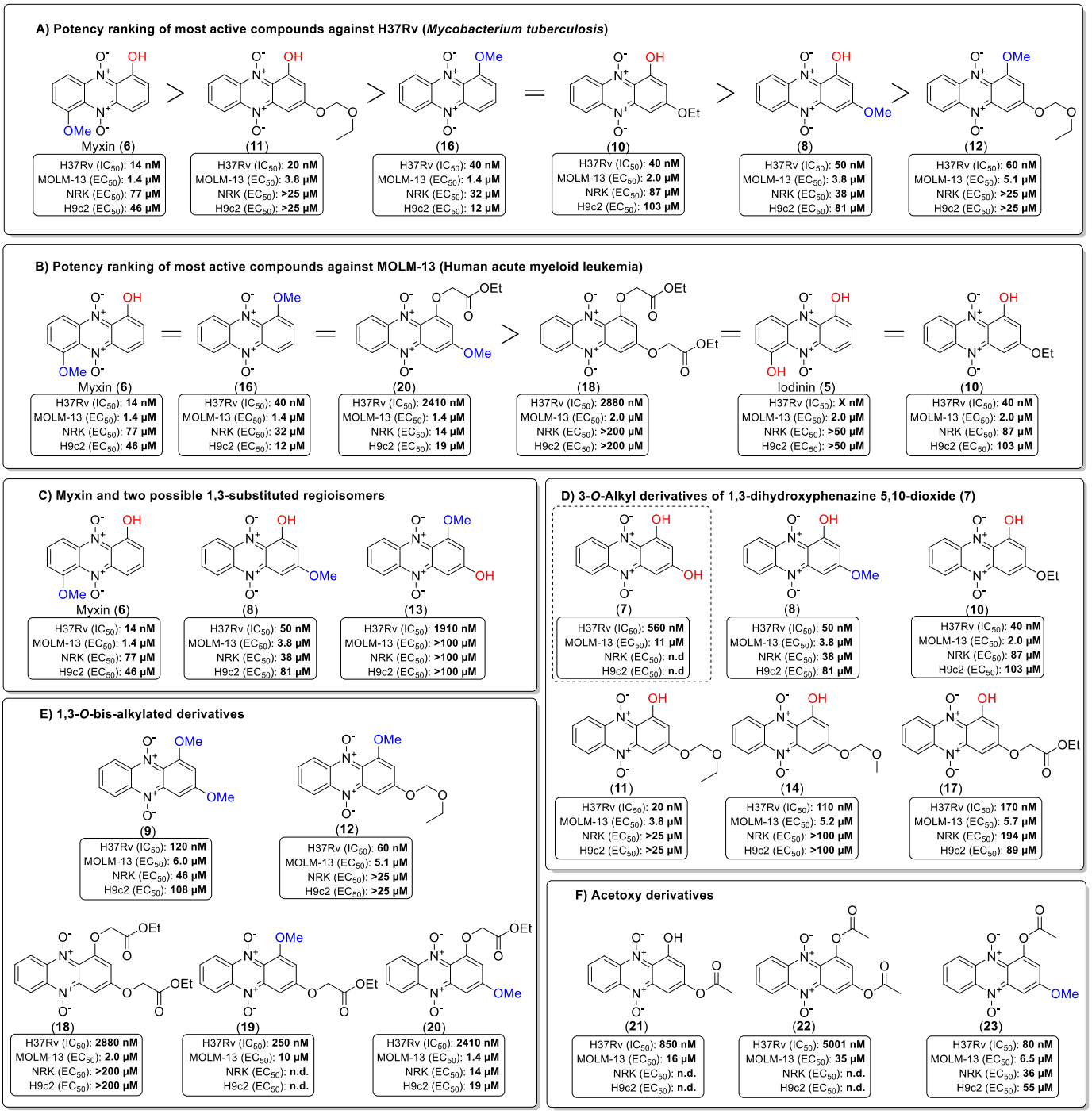

Fig. 2A)-2F). Comparison figures and summary of biological data produced on different types of 1,3-dihydroxyphenazine 5,10-dioxide derivatives.

and the MOLM-13 cells was 0.91 (2-tailed significance <0.001).

The difference in response between the normal cell lines and the *M. tuberculosis* strain H37Rv was even greater than that between MOLM-13 and the normal cell lines (see Supplementary Figs. S–1). The median response for H37Rv was 0.2 μM, whereas the median responses for NRK and H9c2 was 46 and 68 μM, respectively. This is advantageous with respect to antibacterial treatment, since the compounds will be harmful to the bacteria, but will have minimal effects to other cells.

From a broader perspective, the phenazine 5,10-dioxides as a compound class, have proven the capability to inhibit cell growth for a wide variety of different cell types. These include Gram-positive- and Gram-negative bacteria, and fungi [29], also mycobacteria (this work), as well as human cancer cell lines [15,16]. The general consensus is that the primary mode of cytotoxicity-action of phenazine 5,10-dioxides is related to their ability to associate with, and disturb DNA-regulation, involving DNA-intercalation and/or inhibition of topoisomerases. As mentioned in the introduction however, additional mechanistic actions such as ROS production and metal chelation may also play a role and to which extent the analogs also harbor these mechanisms is not known. Thus, assuming the phenazine 5,10-dioxides act primarily on DNA, it can also be concluded that this compound class efficiently crosses various biological membranes and cell walls since this would be required for the compounds to reach their target site of action. Our prior work evaluating passive diffusion using a PAMPA assay showed the

majority of tested phenazine 5,10-dioxides had good cell membrane permeability [16].

2.4. Structure-activity relationship observations

2.4.1. Methylations of hydroxyl groups and impact on biological activity

Methylation of phenol groups was in general associated with higher activity against *Mtb* H37Rv and MOLM-13 cells, but with some exceptions. The natural products iodinin (unmethylated) and myxin (methylated) with respectively an IC_{50} of 170 nM and 14 nM against H37Rv demonstrates the notable impact of this single methylation on antimycobacterial activity (Table 1). Another example demonstrating the impact of methylation on effect against H37Rv was the transformation of 1-hydroxyphenazine 5,10-dioxide (**15**) (IC_{50}: 260 nM) into 1-methoxyphenazine 5,10-dioxide (**16**) (IC_{50}: 40 nM). This methylation also enhanced the activity towards MOLM-13 cells, lowering the IC_{50} from 11 μM for compound **15** to 1.4 μM for compound **16**. In fact, **16** was one of the three most cytotoxic compounds tested on MOLM-13 in this study (Fig. 2B). Although myxin (**6**) and **16** have same IC_{50} values against MOLM-13 (Fig. 2B), myxin has less cytotoxic impact on the non-malignant cell lines NRK and H9c2.

Methylation at the 3-OH position of 1,3-dihydroxyphenazine 5,10-dioxide (**7**) resulted in compound **8**, which displayed significantly enhanced activity towards H37Rv, with the IC_{50} decreasing from 560 to 50 nM (Fig. 2C). Compound **8** was also superior to myxin in activity against the *inhA* + resistant clinical isolate strain (see Table 1). The myxin regioisomer **13** was inefficient against H37Rv (IC_{50}: 1910 nM) and did not possess cytotoxic effects on MOLM-13 up to concentrations of 100 μM. This unexpected outcome was particularly intriguing considering the close structural similarity of **13** and **16**, differing only in a single –OH group at position 3. Consequently, analogs with an alkyl group at position 1 and a phenol –OH at position 3 were not pursued further. Another derivative, 1,3-dimethoxyphenazine 5,10-dioxide (**9**), in which both phenols of **7** were methylated, displayed moderate activity against H37Rv (IC_{50}: 120 nM) and MOLM-13 (IC_{50}: 6.0 μM).

Another regioisomer of iodinin (**5**) was synthesized and tested; 2,3-dihydroxyphenazine 5,10-dioxide (**24**), which exhibited no observed cytotoxic effects on MOLM-13 up to 50 μM concentration. The methylated derivative **25**, also a regioisomer of myxin (**6**), did not prove active either (IC_{50} above 10 μM). Consequently, these compounds (**24** and **25**) were not subjected to further exploration through chemical derivatization due to inactivity. Thus, we could conclude that replacing the –OH phenol from position 1 (compound **7**) to position 2 (compound **24**) results in dramatic decline in biological activity towards the tested cell lines. Further, the results suggest that an oxygen-based substituent is required at position 1 for maintaining potency of the phenazine 5,10-dioxide scaffold.

2.4.2. 3-*O*-alkyl derivatives of 1,3-dihydroxyphenazine 5,10-dioxide (7)

Five derivatives were synthesized from compound **7**, each featuring a substituent at position 3 after alkylation reactions (Fig. 2D). All derivatives (**8**, **10**, **11**, **14**, and **17**) demonstrated increased potency against both H37Rv and MOLM-13 compared to their common synthetic precursor **7**. Overall, these types of compounds were the best performing subclass of 1,3-dihydroxyphenazine 5,10-dioxide (**7**) derivatives, with IC_{50} values ranging between 20 and 170 nM against H37Rv. These molecules had low activity against the non-malignant cell lines NRK and H9c2 (Fig. 2D and Table 1). The five 3-*O*-alkyl derivatives displayed IC_{50} values ranging from 2.0 to 5.7 μM on MOLM-13 with compound **10** being the most potent (IC_{50}: 2.0 μM), comparable to iodinin (**5**, Table 1). Each of these active compounds can be readily synthesized in just two synthetic steps from benzofuroxan.

2.4.3. 1,3-*O*-bis-alkylated derivatives of 1,3-dihydroxyphenazine 5,10-dioxide

Five 1,3-*O*-bisalkylated derivatives were synthesized from compound **7** and screened for activity (Fig. 2E). First, 1,3-dimethoxyphenazine 5,10-dioxide (**9**) exhibited inhibitory activity against both H37Rv (IC_{50}: 120 nM) and MOLM-13 (IC_{50}: 6.0 μM). In comparison to **9**, compound **12**, which differed by a 3-EOM substitution instead of 3-OMe, displayed increased potency against H37Rv (IC_{50}: 60 nM) and MOLM-13 cells (EC_{50}: 5.1 μM). The 1,3-bis(2-ethoxy-2-oxoethoxy) derivative **18** exhibited antileukemic activity equal to iodinin (IC_{50}: 2.0 μM) despite being one of the least effective derivatives against H37Rv (IC_{50}: 2880 nM). This compound was also appealing in terms of antileukemic action due to its low toxicity towards the normal cell lines NRK and H9c2.

The 1-methoxy-3-(2-ethoxy-2-oxoethoxy) derivative **19** and its reversed regioisomer **20** yielded intriguing results, particularly in terms of MOLM-13 cytotoxicity. While **19** demonstrated moderate effects against both H37Rv (IC_{50}: 250 nM) and MOLM-13 (IC_{50}: 10 μM), the reversed regioisomer **20** emerged as a highly cytotoxic agent (IC_{50}: 1.4 μM), showing potency comparable to the most active compounds myxin (**6**) and 1-methoxyphenazine 5,10-dioxide (**16**) on MOLM-13. Additionally, compound **20** exhibited higher cytotoxicity towards NRK and H9c2 compared to the other 1,3-*O*-bisalkylated derivatives outlined in Fig. 2E. In total, four derivatives were tested in this study contain the 2-ethoxy-2-oxoethoxy side chain (compounds **17, 18, 19** and **20**). Of these, only those possessing the 2-ethoxy-2-oxoethoxy side chain in position 1 of the scaffold were highly active against leukemia (**18** and **20**).

2.4.4. Acetylation of phenols

When an acetoxy group was installed into position 3-OH of **7**, the resulting compound (**21**) had modest effect on its activity towards H37Rv and MOLM-13 (Fig. 2F). Subsequently, introducing an acetyl group to both the 1-OH and 3-OH positions of **7** to yield compound **22** led to even lower potency. Notably, **22** exhibited the lowest activity among all compounds tested against H37Rv (IC_{50}: 5001 nM). However, the 1-acetoxy-3-methoxy derivative **23** demonstrated high potency against H37Rv (IC_{50}: 80 nM) and moderate activity against MOLM-13 (IC_{50}: 6.6 μM).

3. Conclusions

In this study, new phenazine 5,10-dioxide derivatives were synthesized and their activity towards *Mtb*, a human AML cell line and two nonmalignant mammalian cell lines (NRK and H9c2) was assessed in vitro. The biological activities of the derivatives were also compared with the natural antineoplastic antibiotics iodinin (**5**) and myxin (**6**). In general, the *Mtb* H37Rv was more sensitive to the analogs compared with the human MOLM-13 AML cell line. A statistically significant difference was also observed in cytotoxicity against the AML cell line and the two normal cell lines NRK and H9c2. There was also a positive correlation revealed between anti-tubercular and anti-leukemic effect. These findings suggest a common mechanism of action in mycobacteria and cancer cells, interruption of normal DNA-metabolism. In particular, the analog series characterized by 1-OH-3-*O*-alkyl substitution revealed high antitubercular potency and low cytotoxic effects on normal cell lines. Two compounds stood out as being potent towards the MOLM-13 cells, but not towards *Mtb* strains, **18** and **20**, demonstrating how the scaffold can be utilized to distinguish between antimicrobial and antineoplastic activities. The 2,3-dihydroxyphenazine 5,10-dioxide scaffold proved ineffective, confirming the importance of an oxygen-based substituent in position 1. Most compounds did not perform as well against clinical isolate *Mtb* strains with resistance-promoting genes. However, 1-OH-3-*O*-akyl derivatives **10** and **11** exhibited high potency against an INH-resistant clinical isolate strain.

This work further strengthens our hypothesis that phenazine 5,10-dioxides should be explored as new alternatives in chemotherapy for *Mtb* and AML. The bioactivity and cytotoxic selectivity of the 1,6-substituted myxin and iodinin was retained with the 1,3-substituted scaffold. To the

best of the authors' knowledge, this study provides the first in vitro structure-activity relationship (SAR) data on phenazine 5,10-dioxides against *Mtb*. However, challenges remain in advancing this class of compounds in terms of drug development. Importantly, two prior in vivo studies have demonstrated the effective administration of phenazine 5,10-dioxides, which increased lifespan or reduced tumor volumes [40, 43], suggesting that this compound class could be effective in vivo. Nonetheless, intensive research is warranted to evaluate the ADMET properties of a newly selected lead, alongside finding efficient methods to improve limited aqueous solubility. For instance, nanoparticle carrier systems such as cyclodextrins or liposomes could be explored in that context, or chemical derivatization prodrugs strategies, exemplified by this groups earlier work for myxin and iodinin analogs [16]. Metabolic stability studies for this class of compounds should also be undertaken, for example in human liver microsomes as a prediction of metabolic stability for the most active substances. Additionally, synergy studies in vitro and in vivo will be crucial, as treatment of diseases like AML and *Mtb* always require a combination of drugs.

This work contributes to bridging the gap in structure-activity relationship studies on phenazine 5,10-dioxides, particularly 1,3-*O*-functionalized phenazines, and further demonstrates the potential of this compound class to offer a new alternative in chemotherapy for *Mtb* or AML.

4. Methods

4.1. General information for synthesis

All purchased reagents were used without further purification. Unless stated otherwise, reactions were performed under N_2 atm. Iodinin (**5**), myxin (**6**) were synthesized as earlier reported by this group [15]. 1-hydroxyphenazine 5,10-dioxide (**15**) was also synthesized in accordance with Viktorsson et al., 2021 [16] based on the Beirut procedure reported by Haddadin et al. [44] Deionized H_2O was used in cases where H_2O is mentioned. For NMR analysis, ^{1}H NMR spectra were recorded on Bruker Avance II instrument at 400 MHz and ^{13}C spectra were recorded 101 MHz respectively. NMR samples were either dissolved in DMSO-d_6 or $CDCl_3$. The NMR spectra were calibrated by the protonated residual solvent as follows: For DMSO-d_6, at 2.50 ppm for the ^{1}H spectra and at 39.52 ppm for the ^{13}C spectra. The $CDCl_3$ spectra were calibrated at 7.26 ppm for ^{1}H and at 77.16 ppm for ^{13}C spectra respectively. Chemical shifts (δ) are reported in parts per million (ppm). Abbreviations are used as follows: s = singlet, d = doublet, t = triplet, q = quartet, m = multiplet, dd = doublets of doublet, bs = broad singlet. Coupling constants (J values) are given in Hertz (Hz). The processing of NMR spectra was performed in MestreNova® software. For visualization of TLC plates after elution, ultraviolet (UV) lamp was used emitting 254 nm or 366 nm. HRMS-ESI spectra were measured with a Bruker micrOTOF-Qmass spectrometer. Before submitting compounds to biological testing, samples were dried for a minimum of 2–3 h on a high vacuum pump at pressure below 1 mbar, or in a dry vacuum oven at 50 °C and 20 mbar. All compounds were assessed >95 % pure by HPLC analysis. HPLC purity analysis was performed on a Dionex UltiMate 3.0 HPLC system, including a column compartment, an autosampler with temperature control, an UltiMate 3000 pump, and an ultraviolet detector. The stationary phase was a Kinetex EVO C18 HPLC column (4.6 × 250 mm, 5 μm; Phenomenex). The mobile phase consisted of 0.1 % formic acid (solvent A) and 0.1 % formic acid in acetonitrile (solvent B). A gradient elution was used: 0–9 min, linear gradient 15–100 % B; 9–10 min, 100 % B; 10–11 min, linear gradient 100–15 % B; 11–14 min, 15 % B. The flowrate was 0.8 mL/min. The UV wavelength was set at 290 nm, and 20 μL was injected for each test solution. HPLC chromatograms, ^{1}H- and ^{13}C- NMR spectra are found in the provided supporting information.

4.2. Synthesis of compounds 7–14 and 16-25

4.2.1. 1,3-Dihydroxyphenazine 5,10-dioxide (7)

In a round bottomed flask, benzofuroxan (11.33 g, 83.24 mmol, 1 eq) and phloroglucinol anhydrous (10.6 g, 84.07 mmol, 1.01 eq) were dispersed in H_2O (600 mL). The mixture was treated with a catalytic amount of NaOH (10 pellets, ~500 mg) and the clear-colored reaction mixture became dark green in a few min, then gradually turning dark purple. The resulting reaction mixture was stirred for 16 h at rt. The reaction was quenched with 2 N HCl. The mixture was filtered using a Büchner funnel and the solid crude material retained was washed with H_2O (~500 mL) and EtOH (~250 mL) or until the crude material (**7**) appeared dark purple with homogenous color. The afforded product material was dried in vacuo, first using a rotavapor, then a vacuum oven at 75 °C for 6 h affording 10.16 g (50 %) of (**7**) as a dark purple solid (99.9 % HPLC purity). ^{1}H NMR (400 MHz, DMSO-d_6) δ 14.96 (s, 1H), 11.20 (s, 1H), 8.54–8.42 (m, 2H), 7.96–7.85 (m, 2H), 7.21 (d, J = 2.5 Hz, 1H), 6.67 (d, J = 2.5 Hz, 1H). ^{13}C NMR (101 MHz, DMSO-d_6) δ 161.7, 154.8, 137.8, 135.5, 131.8, 131.6, 130.7, 122.3, 118.9, 118.6, 105.5, 90.6. (^{1}H, ^{13}C NMR-Spectra in the Supporting information, Fig. S-1, and S-2).

4.2.2. General procedure 1 for the 3-O-alkylation of 1,3-dihydroxyphenazine 5,10-dioxide (7)

This method is based on a similar procedure used for the mono-alkylation of iodinin (**5**) [15]. 1,3-Dihydroxyphenazine 5,10-dioxide (**7**)(2.0 mmol, 1.0 eq), 18-Crown 6 (3 mmol, 1.5 eq) and K_2CO_3 (3 mmol, 1.5 eq) were dispersed in anhydrous DMF (6–10 mL) and the dark green reaction mixture stirred for 30 min at rt. A corresponding alkyl halide (3.0 eq) was added dropwise, typically affording a dark red reaction mixture within 1 h which was stirred for a total of 2–24 h monitored by TLC analysis. The resulting reaction mixture was quenched with a few drops of glacial AcOH and diluted with H_2O. The aqueous phase was extracted with DCM or EtOAc (4 × 30 mL). The combined organic phases were washed with brine (200–500 mL), dried over $MgSO_4$ and filtered before concentrated in vacuo. The obtained crude material was further purified with flash column chromatography on silica gel and in some cases recrystallization as described for each individual compound.

4.2.3. 1-Hydroxy-3-methoxyphenazine 5,10-dioxide (8)

A dry round-bottom flask was charged with 1,3-dihydroxyphenazine 5,10-dioxide (**7**) (5.0 g, 20.47 mmol, 1 eq), K_2CO_3 (4.24 g, 30.71 mmol, 1.5 eq) and 18-Crown-6 (8.11 g, 30.71 mmol, 1.5 eq). The solids were dispersed in anhydrous DMF (120 mL) under inert N_2 atm and shielded from light with aluminum foil. After 30 min of stirring when the resulting mixture had switched color from dark violet towards dark green, a dropwise addition of MeI (1.91 mL, 30.71 mmol, 1.5 eq) was carried out before the mixture was left stirring for an additional period of 16 h at rt. The reaction mixture was concentrated in vacuo, diluted by 200 mL of NH_4Cl (10 % aqueous sol.) and the aqueous phase extracted by EtOAc (2 × 100 mL). The pooled organic phases were dried over $MgSO_4$, filtered, and concentrated. The resulting crude mixture was dry-loaded on silica and further purified by flash column chromatography on silica gel (20–80 % EtOAc/Heptane) to afford 1.75 g (33 %) of **8**, a cherry red solid (95.4 % HPLC purity, chromatograph shown in Supporting information. R_f: 0.32 (50 % EtOAc/Heptane). ^{1}H NMR (400 MHz, $CDCl_3$) δ 14.52 (broad s, 1H), 8.65–8.54 (m, 2H), 7.92–7.70 (m, 2H), 7.37 (d, J = 2.7 Hz, 1H), 6.73 (d, J = 2.5 Hz, 1H), 3.99 (s, 3H). ^{13}C NMR (101 MHz, $CDCl_3$) δ 164.0, 155.0, 138.2, 136.0, 132.5, 131.8, 130.8, 123.8, 119.7, 119.3, 106.6, 88.2, 56.4. HRMS (TOF ES+): Exact mass calculated for $C_{13}H_{11}N_2O_4$ $[M+H]^+$: 259.0719, found 259.0731 (4.6 ppm).

4.2.4. 1,3-Dimethoxyphenazine 5,10-dioxide (9)

MeI (0.12 mL, 1.92 mmol, 5 eq) was added dropwise to a stirring solution of 1-hydroxy-3-methoxyphenazine 5,10-dioxide (**8**) (100 mg,

0.38 mmol, 1 eq), KOtBu (86 mg, 0.77 mmol, 2 eq) and 18-Crown-6 (112 mg, 0.42 mmol, 1.1 eq) in anhydrous THF (10 mL) at 0 °C. The resulting mixture was left stirring overnight gradually reaching rt concentrated in vacuo. The resulting crude was dissolved in H_2O (50 mL, and the organic layer extracted with by EtOAc (2 × 50 mL). Organic phases were pooled, washed with brine (50 mL), dried over $MgSO_4$, filtered, and concentrated in vacuo. The resulting crude was purified by flash column chromatography (10–50 % EtOAc/Heptane) affording 19 mg (24 %) of **9** as red solid (95.9 % HPLC purity). R_f: 0.35 (1:1 EtOAc/Heptane). ^{1}H NMR (400 MHz, DMSO-d_6) δ 8.56–8.44 (m, 2H), 7.94–7.88 (m, 1H), 7.83 (m, 1H), 7.52 (d, J = 2.5 Hz, 1H), 6.90 (d, J = 2.5 Hz, 1H), 3.99 (s, 3H), 3.96 (s, 3H). ^{13}C NMR (101 MHz, DMSO-d_6) δ 161.9, 154.9, 143.7, 143.3, 132.9, 130.2, 126.9, 120.95, 119.68, 103.23, 89.59, 57.60, 56.75. HRMS: Exact mass calculated for $C_{14}H_{13}N_2NaO_4$ $[M+Na]^+$: 295.0683; found 295.0870 (1.6 ppm).

4.2.5. 3-Ethoxy-1-hydroxyphenazine 5,10-dioxide (**10**)

Synthesized according to general procedure 1 using **7** as a starting material (300 mg scale) and Iodoethane as an alkylating agent. Flash column chromatography on silica gel (100 % DCM) gave 102 mg (31 %) of (**10**), a red solid (99.9 % HPLC purity). R_f: 0.70 (100 % DCM). ^{1}H NMR (400 MHz, $CDCl_3$) δ 14.40 (bs, 1H), 8.60–8.49 (m, 2H), 7.83–7.70 (m, 2H), 7.28 (d, J = 2.5 Hz, 1H), 6.66 (d, J = 2.5 Hz, 1H), 4.20 (q, J = 7.0 Hz, 2H), 1.49 (t, J = 7.0 Hz, 3H). ^{13}C NMR (101 MHz, $CDCl_3$) δ 163.3, 154.8, 138.1, 135.8, 132.4, 131.8, 130.6, 123.6, 119.6, 119.2, 106.8, 88.5, 65.0, 14.5. HRMS (TOF ES+): Exact mass calculated for $C_{14}H_{11}N_2NaO_4$ $[M+Na]^+$: 294.0617, found 295.0689 (4.1 ppm).

4.2.6. 3-(Ethoxymethoxy)-1-hydroxyphenazine 5,10-dioxide (**11**)

Synthesized according to general procedure 1 from **7** (318 mg scale) using Chloromethyl ethyl ether (EOM-Cl)(240 μL, 2.58 mmol, 2 eq) as an alkylating agent. Flash column chromatography on silica gel (0–15 % EtOAc/DCM) gave collected fractions of intense red color which were concentrated in vacuo and recrystallized using DCM in hexane. Filtration afforded 216 mg (55 %) of (**11**) as red solid (95.3 % HPLC purity). R_f: 0.85 (5 % MeOH/DCM); ^{1}H NMR (400 MHz, $CDCl_3$) δ 14.61 (s, 1H), 8.67–8.55 (m, 2H), 7.85–7.76 (m, 2H), 7.61 (d, J = 2.5 Hz, 1H), 6.84 (d, J = 2.5 Hz, 1H), 5.41 (s, 2H), 3.78 (q, J = 7.1 Hz, 2H), 1.25 (t, J = 7.1 Hz, 3H). ^{13}C NMR (101 MHz, $CDCl_3$) δ 161.4, 155.3, 138.1, 136.0, 132.7, 131.8, 130.9, 123.7, 119.8, 119.3, 107.0, 93.5, 91.5, 65.4, 15.2. Exact mass calculated for $C_{15}H_{14}N_2NaO_5$[M+Na]$^+$: 302.0903, found: 325.0795 (Error 0.2 ppm).

4.2.7. 3-(Ethoxymethoxy)-1-methoxyphenazine 5,10-dioxide (**12**)

Synthesized according to general procedure 1 using 216 mg of **11** as starting material and dimethyl sulfate (120 μL, 1.32 mmol, 2 eq) as an alkylating agent. Flash column chromatography on silica gel was performed twice (0–15 % EtOAc/DCM). The collected fractions were concentrated in vacuo and recrystallized by using DCM in hexane and filtered to afford 129 mg (65 %) of **12**, an orange solid (93.4 % HPLC purity). R_f: 0.45 (5 % MeOH/DCM) ^{1}H NMR (400 MHz, $CDCl_3$) δ 8.71–8.60 (m, 2H), 7.83 (d, J = 2.5 Hz, 1H), 7.78 (ddd, J = 9.1, 6.8, 1.3 Hz, 1H), 7.71 (ddd, J = 8.8, 6.8, 1.3 Hz, 1H), 6.75 (d, J = 2.5 Hz, 1H), 5.42 (s, 2H), 4.05 (s, 3H), 3.78 (q, J = 7.1 Hz, 2H), 1.25 (t, J = 7.0 Hz, 3H). ^{13}C NMR (101 MHz, $CDCl_3$) δ 159.7, 155.4, 139.2, 136.3, 135.7, 131.8, 130.0, 127.1, 120.6, 119.9, 103.6, 93.7, 93.0, 65.5, 57.3, 15.2. Exact mass calculated for $C_{15}H_{14}N_2NaO_5$[M+Na]$^+$: 316.1059, found: 339.0951(Error 0.9 ppm).

4.2.8. 3-Hydroxy-1-methoxyphenazine 5,10-dioxide (**13**)

A dry round-bottom flask was charged with 3-(ethoxymethoxy)-1-methoxyphenazine 5,10-dioxide (**12**) (129 mg, 0.4 mmol, 1.0 eq), in anhydrous DCM (8 mL) under nitrogen atmosphere at 0 °C. TFA (2 mL) was added dropwise. The resulting mixture had switched color from dark violet towards brownish and the mixture was left stirring for a period of 3 h at 0 °C. The reaction mixture was transferred to ice cold H_2O (50 mL) and neutralized with $NaHCO_3$ (10 % aqueous sol.) and the aqueous phase extracted with DCM (2 × 50 mL). The pooled organic phases were dried with $MgSO_4$, filtered, and concentrated. The resulting crude mixture was dry-loaded on silica and further purified by flash column chromatography on silica gel (0–5% MeOH/DCM) to afford 35 mg (33 %) of (**13**) as a bright cherry-red solid (97.3 % HPLC purity) ^{1}H NMR (400 MHz, DMSO-d_6) δ 11.18 (s, 1H), 8.50–8.40 (m, 2H), 7.87 (ddd, J = 8.6, 6.8, 1.4 Hz, 1H), 7.78 (ddd, J = 8.3, 6.8, 1.3 Hz, 1H), 7.44 (d, J = 2.5 Hz, 1H), 6.80 (d, J = 2.5 Hz, 1H), 3.94 (s, 3H). ^{13}C NMR (101 MHz, DMSO-d_6) δ 160.5, 155.3, 138.7, 135.3, 135.0, 131.8, 129.4, 125.7, 120.0, 119.2, 103.3, 92.2, 57.0. Exact mass calculated for $C_{13}H_{10}N_2NaO_4$[M+Na]$^+$: 281.0531, found: 281.0533 (0.6 ppm).

4.2.9. 1-Hydroxy-3-(methoxymethoxy) phenazine 5,10-dioxide (**14**)

Synthesized according to procedure 1 using 1.0g (4.09 mmol, 1.0 eq) of 1,3-dihydroxyphenazine 5,10-dioxide (**7**) as a starting material and Chloromethyl ethyl ether (MOM-Cl) (0.34 mL, 4.50 mmol, 1.1 eq) as an alkylating agent. Flash column chromatography on silica gel was performed twice (0–15 % EtOAc/DCM). Collected fractions were concentrated in vacuo and recrystallized using DCM in hexane and filtered to afford 0.90 g (76 %) of (**14**) a red solid (99.9 % HPLC purity). R_f: 0.95 (5 % MeOH/DCM); ^{1}H NMR (400 MHz, DMSO-d_6) δ 14.97 (s, 1H), 8.58–8.43 (m, 2H), 8.00–7.88 (m, 2H), 7.43 (d, J = 2.5 Hz, 1H), 6.85 (d, J = 2.6 Hz, 1H), 5.42 (s, 2H), 3.45 (s, 3H). ^{13}C NMR (101 MHz, DMSO-d_6) δ 160.0, 154.7, 137.6, 135.7, 132.3, 132.0, 131.3, 123.4, 119.1, 118.7, 105.6, 94.3, 90.9, 56.2. Exact mass calculated for $C_{14}H_{12}N_2NaO_5$[M+Na]$^+$: 311.0633, found: 311.0638 (Error 1.8 ppm).

4.2.10. 1-Methoxyphenazine 5,10-dioxide (**16**)

Synthesized according to general procedure 1 from **15** (303 mg scale) using MeI (0.24 mL, 3.94 mmol, 3 eq) as an alkylating agent. The crude was purified twice with flash column chromatography (0–2% MeOH/DCM). The pure fractions were combined and concentrated under reduced pressure resulting in 48 mg (15 %) of a bright red solid (99.4 % HPLC purity). R_f: 0.04 (DCM). ^{1}H NMR (400 MHz, $CDCl_3$) δ 8.75–8.63 (m, 2H), 8.33 (dd, J = 9.1, 1.2 Hz, 1H), 7.85–7.73 (m, 2H), 7.66 (dd, J = 9.1, 7.9 Hz, 1H), 7.09 (dd, J = 8.0, 1.3 Hz, 1H), 4.09 (s, 3H). ^{13}C NMR (101 MHz, $CDCl_3$) δ 154.2, 138.4, 137.5, 135.7, 131.8, 131.3, 131.0, 130.1, 120.7, 120.1, 112.0, 110.0, 57.4. Exact mass calculated for $C_{13}H_{10}N_2O_3Na$ $[M+Na]^+$: 265.0584, found 265.0584 (0.1 ppm)

4.2.11. 3-(2-Ethoxy-2-oxoethoxy)-1-hydroxyphenazine 5,10-dioxide (**17**)

Synthesized according to general procedure 1 from compound **7** (300 mg scale) using ethyl bromoacetate (163 μL, 1.47 mmol, 1.2 eq) for an alkylating agent. Flash column chromatography on silica gel was performed twice (0–15 % EtOAc/DCM). The collected fractions were concentrated in vacuo and recrystallized from boiling EtOH and filtered to afford 81 mg (20 %) of (**17**) a red-orange solid (97.5 % HPLC purity). R_f: 0.61 (15 % EtOAc/DCM). ^{1}H NMR (400 MHz, $CDCl_3$) δ 14.58 (s, 1H), 8.68–8.59 (m, 2H), 7.89–7.77 (m, 2H), 7.36 (d, J = 2.7 Hz, 1H), 6.87 (d, J = 2.7 Hz, 1H), 4.83 (s, 2H), 4.31 (q, J = 7.1 Hz, 2H), 1.34 (t, J = 7.1 Hz, 3H). ^{13}C NMR (101 MHz, $CDCl_3$) δ 167.6, 162.1, 155.5, 138.0, 136.1, 132.8, 132.1, 131.1, 124.0, 119.8, 119.4, 106.7, 89.1, 65.6, 62.0, 14.3. HRMS (TOF ES+): Exact mass calculated for $C_{16}H_{14}N_2NaO_6$[M+Na]$^+$: 353.0750, found 353.0744 (1.1 ppm).

4.2.12. 1,3-Bis(2-ethoxy-2-oxoethoxy) phenazine 5,10-dioxide (**18**)

Synthesized according to general procedure 1 from compound **7** (300 mg scale) using ethyl bromoacetate (679 μL, 6.14 mmol, 5.0 eq) as an alkylating agent. Flash column chromatography on silica gel (0–50 % EtOAc/DCM) yielded 70 mg (14 %) of **18** an orange solid (95.4 % HPLC purity). R_f: 0.27 (5 % MeOH/DCM). ^{1}H NMR (400 MHz, $CDCl_3$) δ 8.68–8.52 (m, 2H), 7.85–7.76 (m, 1H), 7.75–7.67 (m, 1H), 7.61 (d, J = 2.6 Hz, 1H), 6.78 (d, J = 2.4 Hz, 1H), 4.86 (s, 2H), 4.80 (s, 2H), 4.29 (q, J = 7.1 Hz, 4H), 1.31 (td, J = 7.1, 5.2 Hz, 6H). ^{13}C NMR (101 MHz,

$CDCl_3$) δ 167.5, 167.4, 160.0, 153.4, 138.9, 136.6, 135.7, 132.2, 130.3, 127.5, 120.7, 119.7, 106.5, 92.1, 67.6, 65.6, 62.0, 61.9, 14.2; (HRMS (TOF ES+): Exact mass calculated for $C_{20}H_{20}N_2NaO_8$ $[M+Na]^+$: 439.1117, found 439.1112 (1.7 ppm).

4.2.13. 3-(2-Ethoxy-2-oxoethoxy)-1-methoxyphenazine 5,10-dioxide (19)

Synthesized according to general procedure 1 from **17** (80 mg scale) using methyl iodide as an alkylating agent. Flash column chromatography on silica gel was performed twice (0–15 % EtOAc/DCM). Collected fractions were concentrated in vacuo, recrystallized from hot EtOH and filtered to afford 25 mg (30 %) of **19** as an orange solid (99.3 % HPLC purity). R_f: 0.35 (15 % EtOAc/DCM). ^{1}H NMR (400 MHz, DMSO-d_6) δ 8.52–8.41 (m, 2H), 7.96–7.86 (m, 1H), 7.86–7.77 (m, 1H), 7.43 (d, J = 2.8 Hz, 1H), 6.94 (d, J = 2.8 Hz, 1H), 5.05 (s, 2H), 4.23 (q, J = 7.1 Hz, 2H), 3.98 (s, 3H), 1.25 (t, J = 7.1 Hz, 3H). ^{13}C NMR (101 MHz, DMSO-d_6) δ 167.9, 159.8, 155.1, 138.4, 135.9, 135.0, 131.9, 130.0, 126.5, 120.0, 119.3, 102.8, 90.3, 65.3, 61.0, 57.2, 14.1; HRMS (TOF ES+): Exact mass calculated for $C_{17}H_{16}N_2NaO_6$ $[M+Na]^+$: 367.0903, found 367.0901 (0.8 ppm).

4.2.14. 1-(2-Ethoxy-2-oxoethoxy)-3-methoxyphenazine 5,10-dioxide (20)

Synthesized according to general procedure 1 from **8** (140 mg scale) using ethyl bromoacetate (62 μL, 0.56 mmol, 1.2 eq) as an alkylating agent. Flash column chromatography on silica gel was performed twice (0–15 % EtOAc/DCM). The collected fractions were concentrated in vacuo and recrystallized from boiling EtOH and filtered to afford 93 mg (50 %) of **20** an orange-red solid (99.9 % HPLC purity). R_f: 0.55 (15 % EtOAc/DCM). ^{1}H NMR (400 MHz, $CDCl_3$) δ 8.71–8.65 (m, 2H), 7.88 (ddd, J = 8.9, 6.9, 1.4 Hz, 1H), 7.76 (ddd, J = 9.1, 6.9, 1.3 Hz, 1H), 7.72 (d, J = 2.6 Hz, 1H), 6.70 (d, J = 2.6 Hz, 1H), 4.86 (s, 2H), 4.32 (q, J = 7.1 Hz, 2H), 4.05 (s, 3H), 1.33 (t, J = 7.1 Hz, 3H). ^{13}C NMR (101 MHz, $CDCl_3$) δ 167.5, 163.0, 153.3, 139.5, 136.6, 135.6, 133.0, 130.1, 127.7, 120.7, 119.7, 106.8, 91.3, 67.7, 62.0, 56.8, 14.3. HRMS (TOF ES+): Exact mass calculated for $C_{17}H_{16}N_2NaO_6[M+Na]^+$: 367.0902, found: 367.0901 (0.4 ppm).

4.2.15. 3-Acetoxy-1-hydroxyphenazine 5,10-dioxide (21)

A dry round bottle flask was charged with 1,3-dihydroxyphenazine 5,10-dioxide (**7**) (300 mg, 1.23 mmol, 1 eq) in anhydrous DCM (20 mL) at 0 °C. Pyridine (1 mL) was added and then acetyl chloride (88 μL, 1.23 mmol, 1 eq) was added dropwise. The resulting reaction mixture was stirred for 16 h at rt. The reaction was monitored by TLC. The resulting mixture was quenched with H_2O (50 mL) and transferred to a separatory funnel. The aqueous phase was extracted with DCM (2 × 50 mL). The pooled organic phases were dried over $MgSO_4$, filtered, and concentrated in vacuo. The resulting crude mixture was dry-loaded on silica and further purified by flash column chromatography on silica gel (20–60 % EtOAc/Heptane) to afford 45 mg (13 %) of **21**, a red-orange solid (100 % HPLC purity). R_f: 0.66 (50 % EtOAc/Heptane). ^{1}H NMR (400 MHz, DMSO-d_6) δ 15.07 (s, 1H), 8.59–8.47 (m, 2H), 8.03–7.93 (m, 2H), 7.69 (d, J = 2.4 Hz, 1H), 7.03 (d, J = 2.4 Hz, 1H), 2.35 (s, 3H). ^{13}C NMR (101 MHz, DMSO-d_6) δ 168.6, 154.7, 153.4, 137.0, 135.9, 133.3, 132.2, 124.8, 119.2, 118.8, 109.1, 100.2, 21.0. HRMS: Exact mass calculated for $C_{14}H_{10}N_2NaO_5$ $[M+Na]^+$: 309.0480; found 309.0482 (0,6 ppm).

4.2.16. 1,3-Diacetoxyphenazine 5,10-dioxide (22)

A dry round bottle flask was charged with **7** (300 mg, 1.23 mmol, 1 eq) in anhydrous DCM (20 mL) at 0 °C. Pyridine (4 mL) was added followed by dropwise addition of acetyl chloride (351 μL, 4.92 mmol, 4 eq). The resulting reaction mixture was stirred for 16 h at rt. The reaction was monitored by TLC. The resulting mixture was quenched with H_2O (50 mL) and transferred to a separatory funnel. The aqueous phase was extracted using DCM (2 × 50 mL). The pooled organic phases were dried over $MgSO_4$, filtered, and concentrated in vacuo. The resulting crude mixture was dry-loaded on silica and further purified by flash column chromatography on silica gel (20–60 % EtOAc/Heptane) to afford 21 mg (10 %) of **22**, a red solid (100 % HPLC purity, chromatograph shown in Supplementary data. R_f: 0.33 (12.5 % EtOAc/DCM). ^{1}H NMR (400 MHz, DMSO-d_6) δ 8.49 (d, J = 8.9 Hz, 1H), 8.06 (d, J = 8.6 Hz, 1H), 7.81 (d, J = 2.3 Hz, 1H), 7.73 (dd, J = 6.8, 2.3 Hz, 1H), 7.66–7.60 (m, 1H), 7.06 (d, J = 2.3 Hz, 1H), 2.45 (s, 3H), 2.31 (s, 3H). ^{13}C NMR (101 MHz, $CDCl_3$) δ 169.7, 168.3, 151.1, 147.3, 145.7, 143.1, 132.2, 130.5, 130.2, 119.1, 118.9, 118.6, 21.3, 21.2. HRMS: Exact mass calculated for $C_{16}H_{12}N_2NaO_6[M+Na]^+$: 351.0593; found 351.0588 (1.8 ppm).

4.2.17. 1-Acetoxy-3-methoxyphenazine 5,10-dioxide (23)

A dry round bottle flask was charged with 1-hydroxy-3-methoxyphenazine 5,10-dioxide (**8**) (207 mg, 0.8 mmol, 1 eq) in anhydrous DCM (20 mL) at 0 °C. Pyridine (1 mL) was added followed by dropwise addition of acetyl chloride (342 μL, 4.8 mmol, 6 eq). After 1 h, a catalytic amount of DMAP was added. The resulting reaction mixture was stirred for 16 h at rt. The reaction was monitored by TLC. The resulting mixture was quenched with H_2O (50 mL) and transferred to a separatory funnel. The aqueous phase was extracted with DCM (2 × 50 mL). The pooled organic phases were dried over $MgSO_4$, filtered, and concentrated in vacuo which afforded oily-reddish crude material. The resulting crude mixture was dry-loaded on silica and further purified by flash column chromatography on silica gel (20–60 % EtOAc/Heptane) to afford 25 mg (11 %) of **23**, a red solid (99.4 % HPLC purity). R_f: 0.45 in 50 % EtOAc/Heptane. ^{1}H NMR (400 MHz, DMSO-d_6) δ 8.62 (dd, J = 8.8, 0.8 Hz, 1H), 8.57–8.54 (m, 1H), 8.05–7.99 (m, 1H), 7.97–7.92 (m, 1H), 7.90 (d, J = 2.8 Hz, 1H), 7.39 (d, J = 2.8 Hz, 1H), 4.09 (s, 3H), 2.47 (s, 3H). ^{13}C NMR (101 MHz, DMSO-d_6) δ 169.2, 160.8, 144.3, 142.0, 138.4, 135.8, 132.5, 131.3, 127.3, 120.0, 119.9, 117.8, 96.0, 57.1, 21.4. HRMS: Exact mass calculated for $C_{15}H_{12}N_2NaO_5[M+Na]^+$: 323.0638; found 323.0638 (0.2 ppm).

4.2.18. 2,3-Dihydroxyphenazine 5,10-dioxide (24)

Benzofuroxan (1.4g, 10.3 mmol) and catechol (1.1g, 10.0 mmol) were transferred to a solution of 15 % KOH in EtOH (50 mL). The resulting mixture was stirred overnight and quenched with dropwise AcOH addition (15 mL). The majority of EtOH was removed in vacuo. The resulting crude material was dispersed in H_2O (100 mL) and filtered. The retained crude material was further washed in the following sequence: H_2O (100 mL), cold EtOH (40 mL), H_2O (50 mL) and EtOH (50 mL). The dark-red material was further dried in vacuo, affording 415 mg (17 %) of **24** and required no further purification. R_f not determined due to high polarity of compound. ^{1}H NMR (400 MHz, DMSO-d_6) δ 11.37 (broad s, 2H), 8.58–8.45 (m, 2H), 7.87–7.80 (m, 2H), 7.78 (s, 2H). 13C NMR (101 MHz, DMSO-d_6) δ 153.5, 133.9, 132.4, 129.8, 119.2, 100.0. Synthesis of the compound has been reported earlier [42]. Exact mass calculated for $C_{12}H_8N_2NaO_4^+[M+Na]^+$: 267.0376, found 267.0379 (0.9 ppm).

4.2.19. 2-Hydroxy-3-methoxyphenazine 5,10-dioxide (25)

In a round bottomed flask, benzofuroxan (0.5 g, 3.7 mmol, 1 eq) and 2-methoxyhydroquinone (0.51 g, 3.7 mmol, 1 eq) were dispersed in H_2O (30 mL). The mixture was treated with a catalytic amount of NaOH (1 pellet, ~50 mg) and the clear-colored reaction mixture became dark green in a few min, then gradually turning towards dark purple. The resulting reaction mixture was stirred for 1 h at rt. The reaction was quenched with 2 M HCl. The resulting mixture was then filtered using a Büchner funnel and the solid crude material retained was washed with H_2O (50 mL) and EtOH (~25 mL) or until the crude material (**25**) appeared orange color. The afforded product material was dried over vacuum and collected. Further drying in an oven at 75 °C for 6 h gave 0.71 g (75 %) of (**25**) a orange solid (93.3 % HPLC purity). ^{1}H NMR (400 MHz, DMSO-d_6) δ 11.50 (s, 1H), 8.63–8.46 (m, 2H), 7.92–7.84 (m, 2H), 7.80 (d, J = 9.3 Hz, 2H), 4.06 (s, 3H). 13C NMR (101 MHz, DMSO-d_6) δ 155.2, 134.8, 134.4, 133.0, 132.3, 130.8, 130.5, 119.8, 119.7, 100.4,

97.8, 57.0. Exact mass calculated for $C_{13}H10N_2NaO_4^+$ $[M+Na]^+$: 281.0537, found 281.0533 (1.5 ppm).

4.3. Microplate Alamar Blue Assay (MABA) protocol

M. tuberculosis H37Rv and drug-resistant cells were inoculated on 7H10+OADC agar plates and incubated at 37 °C. Pure colonies from agar plates were grown to mid-log phase in liquid Middlebrook 7H9 medium supplemented with OADC. Mtb cultures were then exponentially grown and inoculated into Middlebrook 7H9 medium on 96 well plates (about 4×10^5 CFU/mL in 200 μL each well) with escalating concentrations of the testing compounds. Plates were incubated at 37 °C for 1 week before receiving 32.5 μL of a resazurin-tween combination (8:5 ratio of 0.6 mM Resazurin in 1X PBS to 20 % Tween 80) and incubated at 37 °C overnight. The production of fluorescent resorufin aids in determining the MIC (minimum inhibitory concentration) of the testing compounds [45].

4.4. Cytotoxicity tests on mammalian cell lines

All compounds were dissolved in DMSO (D5879, Sigma-Aldrich). The cytotoxicity tests were performed as described in detail in Frazier et al. [46] For cytotoxic testing, MOLM-13 cells (DSMZ, ACC-554) [47] were seeded at 30,000 cells/well, while NRK (ATCC, CRL-6509) and H9c2 (ATCC, CRL-1446) cells were seeded as 5000 cells/well in 96-well microplates with 100 μL medium/well. MOLM-13 cells were cultured in RPMI medium, whereas NRK and H9c2 were cultured in DMEM medium. The media were supplemented with 10 % fetal bovine serum, 0.2 mM L-Glutamine and antibiotics (100 IU/mL penicillin and 0.1 mg/L streptomycin). Cell viability was assessed after 24 h of incubation by use of WST-1 reagent, in accordance with the manufacturer's instructions (Roche Diagnostics, Merck). The cells were then fixed in 2 % buffered formaldehyde (pH 7.4) added the DNA-specific dye Hoechst 33342 (0.01 mg/mL, #14533, Sigma-Aldrich) and nuclear morphology evaluated under UV-microscopy to verify the viability results [48]. IC_{50} values were calculated using a four-parameter regression analyses of the WST-1 signal results using SigmaPlot ver. 14.0 (Systat Software Inc., San Jose, CA, USA) as previously described [16]. The cells were tested for mycoplasma infection using MycoAlert™ during the experiments, and no infection was detected during this study.

CRediT authorship contribution statement

Goraksha Machhindra Khose: Writing – original draft, Data curation. **Siva Krishna Vagolu:** Writing – original draft, Data curation. **Reidun Aesoy:** Writing – original draft, Data curation. **Ísak Máni Stefánsson:** Data curation. **Snorri Geir Ríkharðsson:** Data curation. **Dagmar Ísleifsdóttir:** Data curation. **Maonian Xu:** Data curation. **Håvard Homberset:** Data curation. **Tone Tønjum:** Writing – original draft, Conceptualization. **Pål Rongved:** Conceptualization. **Lars Herfindal:** Writing – review & editing, Writing – original draft, Methodology, Formal analysis, Data curation, Conceptualization. **Elvar Örn Viktorsson:** Writing – review & editing, Writing – original draft, Resources, Project administration, Methodology, Funding acquisition, Formal analysis, Data curation, Conceptualization.

Declaration of competing interest

PR and EÖV are among inventors of a patent No.: US 11,958,842 B2. Current assigne is Adjutec Pharma AS, Norway. PR is an employe of Adjutec Pharma.

Acknowledgements

This project was supported by the Icelandic Research Fund (grant no. 228683–051 to EÖV). We also acknowledge the University of Iceland research fund 2019 and 2022 (for funding to EÖV). Funding was received from the Research Council of Norway (RCN) projects #234506 and #309592, and Norwegian South-Eastern Health Authority project #2013080 to TT. Support was also received from the Norwegian Childhood Cancer Society (Grants # 320001 and #190004; RA and LH). We also thank former MSc.students Guðjón Trausti Skúlason and Haukur Rúnar Magnússon for work on developing synthesis methods.

Supplementary data

Supplementary data to this article can be found online at https://doi.org/10.1016/j.ejmech.2025.117244.

Data availability

Data will be made available on request.

References

[1] Global research agenda for antimicrobial resistance in human health. https://www.who.int/publications/m/item/global-research-agenda-for-antimicrobial-resistance-in-human-health. (Accessed 22 June 2023).
[2] Global tuberculosis report. https://www.who.int/publications/i/item/9789240101531, 2024. (Accessed 30 October 2024).
[3] Treatment for latent TB infection and TB disease. https://www.cdc.gov/tb/topic/treatment/default.htm. (Accessed 15 June 2023).
[4] C.M. Bark, W.H. Boom, J.J. Furin, More tailored approaches to tuberculosis treatment and prevention, Annu. Rev. Med. 75 (2024) 177–188.
[5] N. Guttenberger, W. Blankenfeldt, R. Breinbauer, Recent developments in the isolation, biological function, biosynthesis, and synthesis of phenazine natural products, Bioorg. Med. Chem. 25 (2017) 6149–6166.
[6] J.B. Laursen, J. Nielsen, Phenazine natural products: biosynthesis, synthetic analogues, and biological activity, Chem. Rev. 104 (2004) 1663–1686.
[7] J.M. Turner, A.J. Messenger, Occurrence, biochemistry and physiology of phenazine pigment production, Adv. Microb. Physiol. 27 (1986) 211–275.
[8] A. Price-Whelan, L.E.P. Dietrich, D.K. Newman, Rethinking 'secondary' metabolism: physiological roles for phenazine antibiotics, Nat. Chem. Biol. 2 (2006) 71–78.
[9] C. Liao, X. Huang, Q. Wang, D. Yao, W. Lu, Virulence factors of *Pseudomonas aeruginosa* and antivirulence strategies to combat its drug resistance, Front. Cell. Infect. Microbiol. 12 (2022).
[10] G.W. Lau, D.J. Hassett, H. Ran, F. Kong, The role of pyocyanin in *Pseudomonas aeruginosa infection*, Trends Mol. Med. 10 (2004) 599–606.
[11] J.G. Davis, *Chromobacterium iodinum* (n. sp.), Zentralbl. Bakteriol., Parasitenkunde, Infektionskrankheiten und Hygiene, Abteilung 2, Naturwissenschaftliche: Allgemeine, Lan 100 (1939) 273–276.
[12] I. Tanabe, N. Iio, R. Imanura, T. Matsumoto, A. Obayashi, Studies on the antibiotic action of iodinin, and its reduced from 1,6-phenazinediol, memories of the faculty of agriculture, Kagoshima Uni. 10 (1976) 127, 125.
[13] D.V. Mavrodi, W. Blankenfeldt, L.S. Thomashow, Phenazine compounds in fluorescent *Pseudomonas spp*. Biosynthesis and regulation, Annu. Rev. Phytopathol. 44 (2006) 417–445.
[14] E.A. Peterson, D.C. Gillespie, F.D. Cook, A wide-spectrum antibiotic produced by a species of sorangium, Can. J. Microbiol. 12 (1966) 221–230.
[15] E.Ö. Viktorsson, B. Melling Grøthe, R. Aesoy, M. Sabir, S. Snellingen, A. Prandina, O.A. Høgmoen Åstrand, T. Bonge-Hansen, S.O. Døskeland, L. Herfindal, P. Rongved, Total synthesis and antileukemic evaluations of the phenazine 5,10-dioxide natural products iodinin, myxin and their derivatives, Bioorg. Med. Chem. 25 (2017) 2285–2293.
[16] E.Ö. Viktorsson, R. Aesoy, S. Støa, V. Lekve, S.O. Døskeland, L. Herfindal, P. Rongved, New prodrugs and analogs of the phenazine 5,10-dioxide natural products iodinin and myxin promote selective cytotoxicity towards human acute myeloid leukemia cells, RSC Med. Chem. 12 (2021) 767–778.
[17] Y. Zhao, G. Qian, Y. Ye, S. Wright, H. Chen, Y. Shen, F. Liu, L. Du, Heterocyclic aromatic N-oxidation in the biosynthesis of phenazine antibiotics from lysobacter antibioticus, Org. Lett. 18 (2016) 2495–2498.
[18] S. Sinha, X. Shen, F. Gallazzi, Q. Li, J.W. Zmijewski, J.R. Lancaster, K.S. Gates, Generation of reactive oxygen species mediated by 1-hydroxyphenazine, a virulence factor of *Pseudomonas aeruginosa*, Chem. Res. Toxicol. 28 (2015) 175–181.
[19] U. Hollstein, P.L. Butler, Inhibition of ribonucleic acid synthesis by myxin, Biochemistry 11 (1972) 1345–1350.
[20] U. Hollstein, R.J. Van Gemert, Interaction of phenazines with polydeoxyribonucleotides, Biochemistry 10 (1971) 497–504.
[21] L. Myhren, G. Nygaard, G. Gausdal, H. Sletta, K. Teigen, K. Degnes, K. Zahlsen, A. Brunsvik, Ø. Bruserud, S. Døskeland, F. Selheim, L. Herfindal, Iodinin (1,6-dihydroxyphenazine 5,10-dioxide) from streptosporangium sp. induces apoptosis selectively in myeloid leukemia cell lines and patient cells, mar, Drugs 11 (2013) 332.

[22] B. Briard, P. Bomme, B.E. Lechner, G.L.A. Mislin, V. Lair, M.-C. Prévost, J.-P. Latgé, H. Haas, A. Beauvais, *Pseudomonas aeruginosa* manipulates redox and iron homeostasis of its microbiota partner Aspergillus fumigatus via phenazines, Sci. Rep. 5 (2015) 8220.
[23] R.S. Fraser, J. Creanor, The mechanism of inhibition of ribonucleic acid synthesis by 8-hydroxyquinoline and the antibiotic lomofungin, Biochem. J. 147 (1975) 401.
[24] K. Pavletich, S.C. Kuo, J.O. Lampen, Chelation of divalent cations by lomofungin: role in inhibition of nucleic acid synthesis, Biochem. Biophys. Res. Commun. 60 (1974) 942–950.
[25] V. Prachayasittikul, S. Prachayasittikul, S. Ruchirawat, V. Prachayasittikul, 8-Hydroxyquinolines: a review of their metal chelating properties and medicinal applications, Drug Des. Dev. Ther. 7 (2013) 1157–1178.
[26] B. Balasubramanian, W.K. Pogozelski, T.D. Tullius, DNA strand breaking by the hydroxyl radical is governed by the accessible surface areas of the hydrogen atoms of the DNA backbone, Proc. Natl. Acad. Sci. 95 (1998) 9738–9743.
[27] V. Maria, R. Raymond, Anthracycline cardiotoxicity: prevalence, pathogenesis and treatment, Curr. Cardiol. Rev. 7 (2011) 214–220.
[28] C.E. Bayles, D.E. Hale, A. Konieczny, V.D. Anderson, C.R. Richardson, K.V. Brown, J.T. Nguyen, J. Hecht, N. Schwartz, M.K. Kharel, F. Amissah, T.C. Dowling, S. E. Nybo, Upcycling the anthracyclines: new mechanisms of action, toxicology, and pharmacology, Toxicology and Appl, Pharmacology 459 (2023) 116362.
[29] M. Weigele, G. Maestrone, M. Mitrovic, W. Leimgruber, Antimicrobial agents structurally related to myxin, Antimicrob. Agents Chemother. 10 (1970) 46–49.
[30] U.S. Patent No. 3929790, W. Leimgruber, M. Weigele, Alkylation of Iodinin, 1975.
[31] U.S. Patent No. 3,567,728, J.D. Johnston, M.J. Abuel-haj, Process for the Preparation of Phenazine Di-N-oxides and Related Compounds, 1971.
[32] A.T. Garrison, Y. Abouelhassan, D. Kallifidas, F. Bai, M. Ukhanova, V. Mai, S. Jin, H. Luesch, R.W. Huigens, Halogenated phenazines that potently eradicate biofilms, MRSA persister cells in non-biofilm cultures, and *Mycobacterium tuberculosis*, Angew. Chem. Int. Ed 54 (2015) 14819–14823.
[33] A.T. Garrison, Y. Abouelhassan, D. Kallifidas, H. Tan, Y.S. Kim, S. Jin, H. Luesch, R. W. Huigens III, An efficient buchwald–hartwig/reductive cyclization for the scaffold diversification of halogenated phenazines: potent antibacterial targeting, biofilm eradication, and prodrug exploration, J. Med. Chem. 61 (2018) 3962–3983.
[34] A.T. Garrison, Y. Abouelhassan, V.M. Norwood, D. Kallifidas, F. Bai, M.T. Nguyen, M. Rolfe, G.M. Burch, S. Jin, H. Luesch, R.W. Huigens, Structure–activity relationships of a diverse class of halogenated phenazines that targets persistent, antibiotic-tolerant bacterial biofilms and Mycobacterium tuberculosis, J. Med. Chem. 59 (2016) 3808–3825.
[35] H. Yang, Y. Abouelhassan, G.M. Burch, D. Kallifidas, G. Huang, H. Yousaf, S. Jin, H. Luesch, R.W. Huigens, A highly potent class of halogenated phenazine antibacterial and biofilm-eradicating agents accessed through a modular wohl-aue synthesis, Sci. Rep. 7 (2017) 2003.
[36] M. Conda-Sheridan, L. Marler, E.-J. Park, T.P. Kondratyuk, K. Jermihov, A. D. Mesecar, J.M. Pezzuto, R.N. Asolkar, W. Fenical, M. Cushman, Potential chemopreventive agents based on the structure of the lead compound 2-Bromo-1-hydroxyphenazine, isolated from streptomyces species, strain CNS284, J. Med. Chem. 53 (2010) 8688–8699.
[37] H. Cerecetto, M. González, M.L. Lavaggi, A. Azqueta, A. López de Cerain, A. Monge, Phenazine 5,10-dioxide derivatives as hypoxic selective cytotoxins, J. Med. Chem. 48 (2005) 21–23.
[38] H. Cerecetto, M. Gonzalez, M.L. Lavaggi, M.A. Aravena, C. Rigol, C. Olea-Azar, A. Azqueta, A.L.d. Cerain, A. Monge, A.M. Bruno, Phenazine 5,10-dioxide derivatives as hypoxic selective cytotoxins: Part II. Structure-activity relationship studies, Med. Chem. 2 (2006) 511–521.
[39] M. Gonda, M. Nieves, E. Nunes, A. López de Ceráin, A. Monge, M.L. Lavaggi, M. González, H. Cerecetto, N. Phenazine, N′-dioxide scaffold as selective hypoxic cytotoxin pharmacophore. Structural modifications looking for further DNA topoisomerase II-inhibition activity, MedChemComm 4 (2013) 595–607.
[40] M. Lavaggi, M. Cabrera, C. Pintos, C. Arredondo, G. Pachon, J. Rodriguez, S. Raymondo, J. Pacheco, M. Cascante, C. Olea-Azar, A. Cerain, A. Monge, H. Cerecetto, M. Gonzalez, Novel phenazine 5,10-dioxides release •OH in simulated hypoxia and induce reduction of tumour volume in vivo, ISRN Pharmacol. 2011 (2011) 11.
[41] M.L. Lavaggi, M. Cabrera, M. González, H. Cerecetto, Differential enzymatic reductions governing the differential hypoxia-selective cytotoxicities of phenazine 5,10-dioxides, Chem. Res. Toxicol. 21 (2008) 1900–1906.
[42] M.J.A. El-Haj, B.W. Dominy, J.D. Johnston, M.J. Haddadin, C.H. Issidorides, New route to phenazine 5,10-dioxides and related compounds, J. Org. Chem. 37 (1972) 589–593.
[43] K. Hano, H. Iwata, K. Nakajima, Studies on the anticancer activity of phenazine derivatives, Chem. Pharm. Bull. 13 (1965) 107–113.
[44] C.H. Issidorides, M.A. Atfah, J.J. Sabounji, A.R. Sidani, M.J. Haddadin, Application of 1,2-diketones in the synthesis of phenazine oxides, Tetrahedron 34 (1978) 217–221.
[45] E. Koçak Aslan, V.S. Krishna, S.J. Armaković, S. Armaković, O. Şahin, T. Tønjum, M.G. Gündüz, Linking azoles to isoniazid via hydrazone bridge: synthesis, crystal structure determination, antitubercular evaluation and computational studies, J. Mol. Liq. 354 (2022) 118873.
[46] T. Frazier, E. Pereira, R. Aesoy, L. Nauton, F. Giraud, L. Herfindal, F. Anizon, P. Moreau, Synthesis, kinase inhibition and anti-leukemic activities of diversely substituted indolopyrazolocarbazoles, Eur. J. Med. Chem. 269 (2024) 116352.
[47] Y. Matsuo, R.A.F. MacLeod, C.C. Uphoff, H.G. Drexler, C. Nishizaki, Y. Katayama, G. Kimura, N. Fujii, E. Omoto, M. Harada, K. Orita, Two acute monocytic leukemia (AML-M5a) cell lines (MOLM-13 and MOLM-14) with interclonal phenotypic heterogeneity showing MLL-AF9 fusion resulting from an occult chromosome insertion, ins(11;9)(q23;p22p23), Leukemia 11 (1997) 1469–1477.
[48] L. Myhren, I.M. Nilssen, V. Nicolas, S.O. Døskeland, G. Barratt, L. Herfindal, Efficacy of multi-functional liposomes containing daunorubicin and emetine for treatment of acute myeloid leukaemia, Eur. J. Pharm. Biopharm. 88 (2014) 186–193.